JOURNAL OF CATALYSIS 130, 359–373 (1991)

Morphology and Site Blocking Effects on Chemisorption Properties and Reactivity of Pt/TiO_2 and Sulfided Pt/Al_2O_3 Catalysts

LAURENT BONNEVIOT* AND GARY L. HALLER†

*Department de Chimie, Laval Université, Ste-Foy, Quebec, G1K 7P4, Canada; and, †Department of Chemical Engineering, Yale University, New Haven, Connecticut 06520

Received December 19, 1988; revised January 1, 1991

Hydrogen and carbon monoxide chemisorption as well as *n*-butane isomerization and hydrogenolysis were performed on Pt/η-Al_2O_3, taken as a reference, on sulfided Pt/η-Al_2O_3 and on Pt/TiO_2 catalysts reduced either at low (513 K), medium (573 K), or high (773 K) temperature. The poisoning by sulfur or TiO_x decoration leads to a complete loss of irreversible hydrogen or carbon monoxide chemisorption and a depression by three orders of magnitude of the original platinum surface activity. In both cases, the surface inhibition effect is similar and conveniently shown, for reactivity, on compensation plots. Since sulfur adatoms or TiO_x fragments are supposed to induce a transfer of electrons in the opposite direction, one must conclude that both inhibitions are mainly due to geometric effects. In both cases, the surface inhibition appears to take place in two steps and can be reversed by oxygen treatment. First, an apparent flattening of the particles that leads to less active, low index planes exposure to reactants and to a compensation effect is suggested. This occurs at high temperature on Pt/η-Al_2O_3 and at medium temperature in the presence of sulfur or TiO_2. Then, following a high temperature reduction, the second step, which is responsible for the major part of the inhibition, takes place by simple site blocking by sulfur or TiO_x moieties and does not lead to compensation.

INTRODUCTION

A high temperature reduction of group VIII metals supported on TiO_2 suppresses the hydrogen chemisorption capacity of the metal and may deactivate their catalytic sites for some reactions. This has been called a strong metal support interaction (SMSI) by Tauster et al. (*1*). The electronic model, invoked to explain this effect in the beginning, was quickly called into question (*2*) and a geometric model, involving a decoration of the particles by the support, now prevails (*3–7*). Of course, we refer to the effect that appears to dominate since electronic and geometric models are not mutually exlusive. Model system studies have convincingly demonstrated that TiO_x moieties at the surface of a metal on Rh/TiO_2 (*5, 6*) and Pt/TiO_2 (*8*) account for the suppression of chemisorption caused by SMSI. A positive effect on the catalytic activity has also been observed in the case of CO hydrogenation (*9*). However, in this reaction the dissociation of CO molecules produces oxygen atoms which can reverse SMSI by reoxidation of the catalysts (*10*). Therefore, enhancement of activity cannot be unambiguously attributed to SMSI (*11*). A more significant finding for SMSI is the enhancement of graphite hydrogenation (no O atoms involved) under SMSI conditions of reaction found by Baker *et al.* (*12*) for the Pt/TiO_2 system compared to Pt particles only.

As far as hydrogenolysis is concerned, deactivation may be considered as a desirable consequence of SMSI since this reaction is an undesirable side reaction in the reforming process. In fact, for the most active metals for this reaction, rhodium and iridium, a drastic drop in activity by four orders of magnitude accompanies SMSI. After suppression of hydrogenolysis activity, isomerization and dehydrogenation of alkanes can be observed on these metals (*13*). For platinum, which is less active for hydrogenolysis (*14*) and already active in isomerization in the normal state, one can

0021-9517/91 $3.00

expect a more pronounced preference of the selectivity toward isomerization and dehydrogenation. This goal is reached on practical reforming catalysts Pt/Al_2O_3 and $Pt–Re/Al_2O_3$, by adding sulfur (*15*). The addition of sulfur and rhenium to platinum has been interpreted to result in the division of the platinum surface into small sulfur-free ensembles, separated by rhenium atoms covered by sulfur (*16*). A somewhat similar situation must occur when Pt particles are, at least partially, covered by TiO_x fragments in the SMSI state. In contrast to the similar geometric effect described above, the electronic effect is expected to be very different. The sulfur adatoms are negatively charged due to an electron transfer from platinum to sulfur (*17*) leading to a $Pt^{\delta+}–S^{\delta}$ system. Moieties of TiO_x cover the particles and are believed to induce an electron transfer toward the metal leading to a $Pt^{\delta-}–Ti^{m+}$ system, the reverse of that for sulfur chemisorption. Using different electron spectroscopies, Sadeghi and Henrich have recently confirmed this electron transfer toward the metal when the metal is Rh (*18*). They showed that this charge transfer does not lead to a large-scale suppression of CO adsorption, although local bonding effects described theoretically (*19–21*) which may perturb chemisorption are not ruled out by the results of Sadeghi and Henrich.

An EPR investigation of the Pt/TiO_2 catalysts reduced at various temperatures was reported in a previous paper where we characterized four different signals due to Ti^{3+} ions (*22*). One of these signals, obtained at very low temperature (17 K) had not been characterized previously and was attributed to Ti^{3+} ions in contact with platinum and could account for the suboxide TiO_x species which migrates on the metal surface.

In this work, we report a comparative investigation of the effect of SMSI in Pt/TiO_2 catalysts and of the effect of sulfur poisoning in Pt/Al_2O_3 catalysts on the nature of hydrogen and carbon monoxide chemisorption and on the activity and selectivity of these catalysts for hydrogenolysis of *n*-butane. Total and reversible hydrogen and CO uptakes were measured for each gas on the Pt/TiO_2 system to characterize the surface inhibition. The hydrogenolysis selectivities to propane (C_3), ethane (C_2), and methane (C_1), and isomerization are used as a fingerprint for the comparison of the two effects. To minimize the influence of the particle size, which is not our interest here, the metal dispersion of the Pt/Al_2O_3 catalysts was bracketed between those of the Pt/TiO_2 catalysts. The goal is to assess the relative importance of the electronic effect versus the geometric effect on the reactivity of platinum, with the assumption that the electronic effect is expected to be quite different in the two cases, as mentioned above, but the geometric consequences are expected to be similar.

EXPERIMENTAL SECTION

Titania-supported platinum catalysts were prepared by cation exchange of Degussa P 25 TiO_2 with a solution of $Pt(NH_3)_4(NO_3)_2$ provided by Alfa/Ventron. The procedure is described in detail in a preceding paper (*22*) and is similar to the procedure used for Rh/TiO_2 and Ir/TiO_2 catalysts (*13*). The Pt loadings were 0.44 and 1.0 wt%, respectively. Subsequently, the standard reduction treatment was carried out with initial reduction at 773 K in a pure H_2 flow at a rate of 50 cm^3/min with a heating rate of 3 K/min. A 5 wt% Pt/Al_2O_3 catalyst was prepared by incipient wetness impregnation of η-Al_2O_3 with a solution of H_2PtCl_6 provided by Alfa/Ventron. The η-Al_2O_3 was obtained by calcination of β-Al_2O_3 at 823 K for 3 h. The impregnated catalyst was oxidized at 773 K, reduced at 773 K, and passivated in air at room temperature before storage in a desiccator. The sulfided Pt/Al_2O_3 catalyst, containing 1 wt% S, was obtained by incipient wetness impregnation of the 5 wt% Pt/Al_2O_3 reduced catalyst with ammonium sulfate in aqueous solution (the S/Pt molar ratio equals 0.82).

The samples were stored in a desiccator at 298 K. For each new experiment, the

oxidized catalysts were reduced in pure H_2 (same heating rate, same flow rate) from 298 K to a temperature indicated as follows: (O673, R773) for an oxidation at 673 K, and a reduction at 773 K, respectively, with a final temperature maintained in both cases for two h. A second low temperature reduction (LTR, 513 K) or medium temperature reduction (MTR, 573 K) catalyst is obtained after high temperature reduction (HTR, 773 K) followed by a new oxidation–reduction cycle *in situ*. They are referred to as LTR-II or MTR-II, respectively, to distinguish them from the first reduction referred to as LTR-I or MTR-I.

The gases were supplied by New England Welding Company and all were 99.99% pure. Hydrogen was further purified through a palladium diffuser, and CO by passing it through a reduced Cr/SiO_2 catalyst. Gas pressures were measured with a Baratron pressure gauge in a conventional Pyrex volumetric system; the vacuum provided by an oil diffusion pump was regularly at 10^{-3} Pa. For each adsorption isotherm, three points were taken on the plateau of the adsorption curve at about 6.67, 13.3, and 20 kPa and the equilibration times were 15, 1, and 1 h, respectively, after the introduction of the gas. The H/Pt and CO/Pt ratios were calculated at zero pressure by extrapolation. Hydrogen and CO uptakes were measured at 295 K (room temperature) in the following sequence for each sample: the first H_2 isotherm after evacuation of the catalyst for 1 h at the temperature of reduction, a second H_2 isotherm after evacuation at 295 K for 30 min, followed by a second evacuation at the temperature of reduction for 30 min, then followed by a first CO isotherm and a second one after evacuation at 295 K for 30 min. The hydrogen uptake was found to be identical after a first evacuation of H_2 at the temperature of reduction or after a cycle of adsorption at room temperature and desorption at the temperature of reduction. The subsequent CO adsorptions taken at the latter conditions can thus be considered as the same as if they were directly taken without previous H_2 chemisorption experiments.

The reactions were performed in a steady-state flow mode in a packed bed reactor as described previously (*23*). At a given temperature, the rate was measured twice and each Arrhenius plot was based on four different temperature measurements taken in order of increasing temperature. After this set of measurements, a fifth, and sometimes a sixth, measurement was taken by decreasing the temperature to check the reversibility and the reaction self-poisoning. The reported turnover frequency, whatever the reduction temperature of the catalysts, is based on a site density measured by hydrogen chemisorption given by the first hydrogen isotherm on a sample reduced at low temperature 513 K when the support was TiO_2. This is justified by the presence of SMSI at higher reduction temperatures which suppresses the hydrogen chemisorption on the metal as shown in this work (vide infra) in line with previous studies on Rh/TiO_2 (*24*). Temperature was monitored with a iron-constantan thermocouple located in the catalyst bed and programmed with a temperature controller which allows a stabilization of the temperature within 0.5 K. Hydrogen and *n*-butane flows were independently measured and controlled by mass flowmeters placed in parallel. The reactant mixture was held at a ratio of 1 : 20 (*n*-butane : hydrogen). The total flow rate was 2.28 liter/h and constant activity levels were obtained after 30 min on stream. The products were analyzed by an on-line gas chromatograph equipped with a packed column (Carbopak C/0.19% picric acid) and a flame ionization detector). Hydrogen of 99.995% purity was diffused through a Pd–Ag cell, as for adsorption studies, and MG Sci. Gases Inst. Grade *n*-butane was used as reactant.

RESULTS

Hydrogen and Carbon Monoxide Chemisorption

Hydrogen and carbon monoxide uptake results are depicted as a function of different

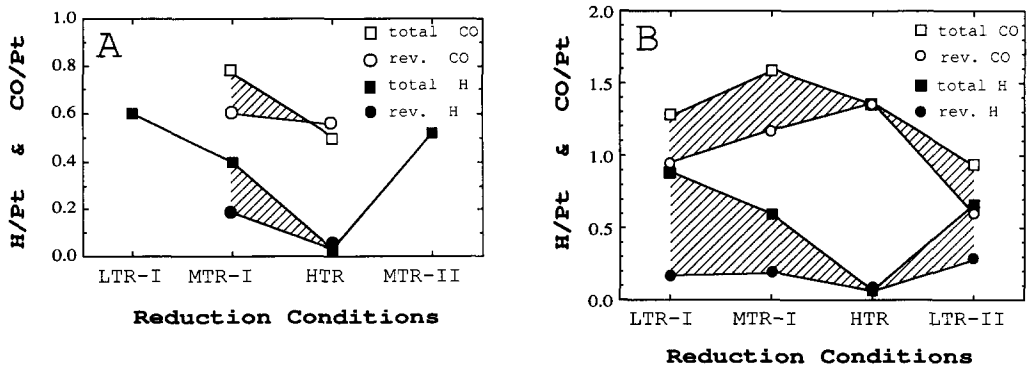

FIG. 1. Measured H/Pt and CO/Pt for total adsorption (■ and □, respectively) and for reversible adsorption (● and ○, respectively) (A) on 1 wt% Pt/TiO_2 and (B) on 0.44 wt% Pt/TiO_2 as a function of the reduction conditions, LTR = 513 K, MTR = 573 K, and HTR = 773 K reduction temperatures.

reduction conditions in Fig. 1 for Pt/TiO_2 catalysts and in Fig. 2 for Pt/Al_2O_3 catalyst. The first hydrogen uptake, taken after reduction at 513 K (LTR) and 573 K (MTR) for Pt/TiO_2 and Pt/Al_2O_3 systems, respectively, is designated the metal dispersion. While it is recognized that subsequent treatments may result in changes in dispersion, previous work suggests that these are modest (*1*) and, in any case, they cannot be separated from SMSI and sulfur poisoning effects by chemisorption alone. With an 0.80 H/Pt ratio, 5 wt% Pt/Al_2O_3 catalyst has a metal dispersion that lies in between the metal dispersion of 1 wt% and 0.44 wt% Pt/TiO_2 catalysts with H/Pt = 0.60 and 0.89, respectively.

After evacuation for 30 min at 295 K, a second hydrogen uptake was performed and found to be smaller than the first one. This is due to the presence of irreversibly adsorbed hydrogen, the second uptake titrating the reversible part. In what follows, the first uptake is designated the total adsorption, the second uptake the reversible adsorption, and the difference between these two, the irreversible adsorption. The same nomenclature is applied to CO adsorption, which was calculated the same way as for hydrogen.

From Fig. 1, it clearly appears that the CO/Pt is always greater than H/Pt for Pt/TiO_2 catalysts while on Fig. 2 a reverse situation is observed for Pt/Al_2O_3 catalyst,

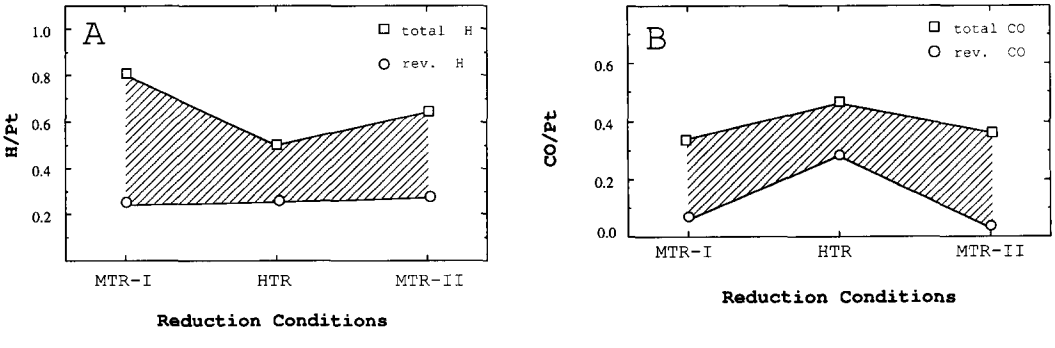

FIG. 2. (A) Measured H/Pt for total adsorption and reversible adsorption (■ and ●, respectively) on the 5 wt% Pt/Al_2O_3 as a function of the reduction conditions.

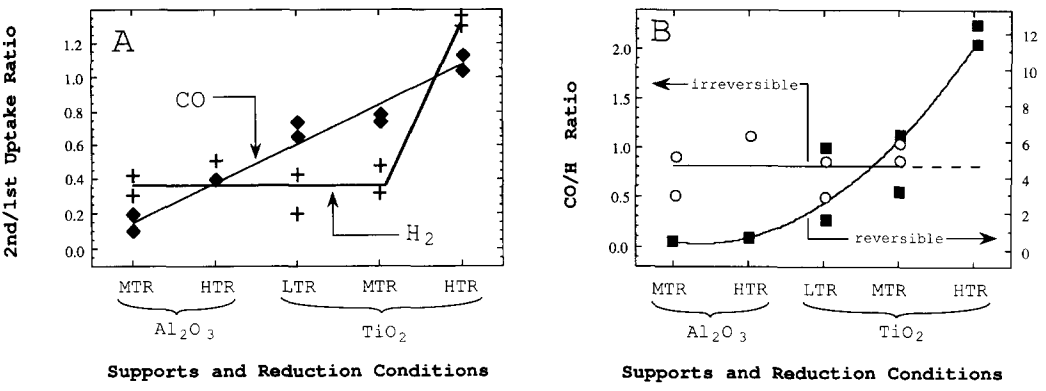

FIG. 3. (A) A plot of first to second uptakes (total to reversible uptakes for CO and hydrogen (◆ and + respectively) as a function of support and support pretreatment. (B) Measured CO/H ratio for reversible and irreversible adsorption (■ and ○, respectively) as a function of support and support pretreatment.

whatever the temperature of reduction. For 0.44 wt% Pt/TiO_2 catalysts the CO uptake even increases after 573 K reduction. The HTR Pt/Al_2O_3 catalyst neither exhibits an increase of the CO uptake nor undergoes a significant depression of the hydrogen uptake. A more striking point concerns the nature of the adsorption for both gases; after HTR, Pt/TiO_2 catalysts have a second uptake equal to the first one within experimental accuracy. This indicates that the adsorption is completely reversible. The shaded area in Fig. 1 and 2 points out the irreversible part of hydrogen and carbon monoxide adsorption which disappears in the SMSI state.

In Fig. 3a, the ratio of the second to the first (reversible to total) uptake for CO and H_2 is plotted versus the nature of the support and the reduction temperature. The straight lines are drawn to indicate the trend. It appears that either a change from Al_2O_3 to TiO_2 or an increase of reduction temperature increases the reversible part of CO adsorption as follows: 0.18, 0.39, 0.7, 0.75, and 1.1 for Al_2O_3-MTR, Al_2O_3-HTR, TiO_2-LTR, TiO_2-MTR, and TiO_2-HTR, respectively. On the contrary, the hydrogen chemisorption turns out to be always about 40% reversible at room temperature except for HTR of Pt/TiO_2. Nevertheless, one notes that the reversible contribution is lower for Al_2O_3-MTR-I (30%) and TiO_2-LTR-I (20%) which could be due to the incomplete reduction of platinum. One can conclude that irreversible adsorption mainly characterizes the metal while the reversible part is, for the most part, due to the support, particularly for CO.

Figure 3b depicts the evolution of the CO/H ratio versus support and reduction temperatures in a presentation similar to Fig. 3a. One notes that the CO/H ratio calculated from the total uptakes varies from 0.43 to 1.08 on Al_2O_3 in MTR and HTR conditions, respectively, and from 0.5 to 2–2.7 and 17 in LTR, MTR, and HTR conditions, respectively. The ratio of the irreversible part of the adsorption at room temperature does not vary as much as the ratio of the overall chemisorption. For the irreversible part, the ratio is roughly one. Nevertheless, on a closer examination of these ratios, it appears that the value is rather low (0.5) on Al_2O_3-MTR-I as well as on TiO_2-LTR-I. On 0.44 wt% Pt/TiO_2 and on Al_2O_3 in MTR and HTR conditions, respectively, CO/H based on irreversible adsorption increases up to 1.05 and 1.08, respectively. After a high temperature reduction–oxidation–low reduction cycle the ratio is 0.85 on both supports. This intermediate value indicates that

TABLE 1

Activation Energy[a] of the Reactions of *n*-Butane over 0.44 wt% Pt/TiO_2 Catalyst (Samples 1, 2, and 3) and over 5.0 wt% Pt/Al_2O_3 Catalyst, Unsulfided (Sample 4 and 5) or Sulfided (Samples 6, 7, 8, and 9)

Spl. No.	Reduction conditions	Hydrogenolysis			Isomerization isobutane	Dehydrogenation				T^b
		CH_4	C_2H_6	C_3H_8		1-But.	*trans*. -But.	*cis* -But.	Total	
1	MTR-I[c]	162	195	163	196	—	—	—	170	585
2	HTR[c]	159	193	168	187	[d]	141	127	173	665
3	MTR-II[c]	156	208	169	138	[e]	[e]	[e]	173	589
	$(\Delta E_a)^a$	+1.5	−4	+4.5	+3	—	—	—	+4	
4	MTR[f]	185	204	197	271	—	—	—	198	538
5	HTR[f]	158	196	165	196	—	—	—	174	549
	$(\Delta E_a)^a$	−27	−8	−32	−75	—	—		−19	
6	MTR-I-Sulfided[g]	171	192	173	183	[d]	119	122	179	656
7	HTR-I-Sulfided	169	199	171	187	[d]	127	116	180	647
8	MTR-II-Sulfided	159	216	169	186	—	—	—	177	547
9	HTR-II-Sulfided	142	179	166	202	[d]	140	104	160	611

[a] Activation energy in kJ/mol, $\Delta E_a = E_a(\text{HTR}) - [E_a(\text{LTR-I}) + E_a(\text{LTR-II}]/2$.

[b] T, reaction temperature in K which corresponds to 1% *n*-butane conversion, temperature range of the reaction = $T \pm 20$ K.

[c] MTR (HTR): reduction at 623 (773) K for 1 h; overall conversion range = 2.4–9.0 (2.3–6.5)%.

[d] 1-Butene is always formed. At low conversion, its peak is not resolved due to a strong overlap with the *n*-butane peak. At high conversion, one compares the conversion of 1-butene with the conversion of other butenes. In all cases, the relative concentration of butenes corresponds to their thermodynamic stability.

[e] At 663 K dehydrogenation is undetectable on the LTR-II Pt/TiO_2 where the actual overall conversion of *n*-butane is 20.2%. By comparison at the same temperature, a HTR catalyst exhibits 0.6% conversion in the dehydrogenation reaction.

[f] MTR (HTR): reduction at 573 (773) K for 1 h; overall conversion range = 1.5–8.3 (1.4–9.4)%.

[g] The sulfided catalysts are prepared from the oxidized unsulfided catalysts and are sequentially reduced at medium or high temperature and a second medium or high temperatures as indicated in Footnote *f*. They correspond to MTR-I-sulfided, HTR-I-sulfided, MTR-II, sulfided, and HTR-II-sulfided, respectively.

the initial state is not completely recovered. This ratio, which probably depends on the nature of the exposed face of the metal, suggests that the morphology of the particles changes at lower temperature on TiO_2 than on Al_2O_3 and is not completely reversed by the oxidation–low temperature reduction cycle.

n-Butane Catalytic Reactions

Tables 1 and 2 report apparent activation energies and turnover frequencies for *n*-butane reactions on the sulfided or unsulfided catalysts treated at different temperatures. In Table 1, reaction temperatures are reported for a 1% *n*-butane overall conversion. In Table 2, all the turnover frequencies were calculated at the same intermediate temperature of 600 K to allow comparison among catalyst activities. Nevertheless, one should be careful of direct comparison of turnover frequencies when the actual reaction temperature and the activation energies are very different. This is particularly true for isomerization (I), for which the activation energy varies to a large extent from one catalyst to another (138 to 271 kJ mol^{-1}), and also for selectivity in reactions with a very different E_a for a given catalyst. Therefore, selectivities were calculated in the range of reaction temperature at 1% *n*-butane overall conversion, i.e., at the different temperatures reported in Table 1. No data were taken after low temperature reduction since the low reactivity of platinum requires at least a medium temperature to be effec-

TABLE 2

Turnover Frequency[a] of the Reactions of *n*-Butane over 0.44 wt% Pt/TiO_2 Catalyst (Samples 1, 2, and 3) and over 5.0 wt% Pt/Al_2O_3 Catalyst, Unsulfided (Samples 4 and 5) or Sulfided (Samples 6, 7, 8, and 9)

Spl. No.	Reduction conditions	H[b]	I[b]	D[b]	Parameters of Selectivity[c]			
					S(I)	S(D)	C_3/C_2	C_1/C_3
1	MTR-I[d]	0.50	2.4×10^{-2}	0.0	0.040	0.0	4.4	1.0
2	HTR[d]	8.5×10^{-3}	8.4×10^{-4}	6.7×10^{-3}	0.09	0.26	2.4	1.1
3	MTR-II[d]	0.44	0.12	0.0	0.23	0.0	4.5	1.7
4	MTR[e]	6.7	2.0	—	0.051	—	0.75	1.3
5	HTR[e]	1.7	0.31	—	0.10	—	2.0	1.1
6	MTR-I-Sulfided[f]	3.6×10^{-3}	1.4×10^{-3}	3.2×10^{-3}	0.25	0.19	1.6	1.3
7	HTR-I-Sulfided	1.1×10^{-2}	3.9×10^{-3}	3.0×10^{-3}	0.28	0.08	2.0	1.1
8	MTR-II-Sulfided	2.5	0.041	—	0.014	—	3.2	1.2
9	HTR-II-Sulfided	3.8×10^{-2}	3.5×10^{-3}	2.9×10^{-3}	0.09	0.08	1.8	1.4

[a] Turnover frequency, TOF, at 600 K in mol · s^{-1}. $site^{-1} \times 10^{-2}$.
[b] H, hydrogenolysis; I, isomerization (isobutane); D, dehydrogenation (butenes).
[c] Selectivities are calculated at 1% *n*-butane conversion, i.e., at the temperature given in Table 1.
[d] As Footnote *c* in Table 1.
[e] As Footnote *f* in Table 1.
[f] As Footnote *g* in Table 1.

tively measured below the reduction temperature.

The three first lines of the two tables concern the 0.44 wt% Pt/TiO_2 catalyst treated at MTR and HTR conditions (samples 1–3). The activation energies for hydrogenolysis stay approximately unchanged after MTR or HTR ($\Delta E_a \leq 5$ kJ mol^{-1}). They are about 160 kJ mol^{-1} for the terminal carbon–carbon rupture (see C_1 and C_3 products). Isomerization (I) follows the same trend as hydrogenolysis with the E_a of 195 kJ mol^{-1} close to the E_a of the middle-chain carbon–carbon rupture except after MTR-II. Dehydrogenation occurs under our reaction conditions only after HTR and characterizes the SMSI state of the Pt/TiO_2 catalyst. The major product is the *trans*-2-butene and the product distribution roughly follows the thermodynamic stability of the isomers. The activation energy for dehydrogenation lies in a 120–140 kJ mol^{-1} range.

Strong metal-support interaction after HTR produces a drop in the hydrogenolysis rate by about 50 times its value after MTR. The selectivity for C–C terminal bond rupture decreases under the SMSI condition as indicated by the C_3/C_2 ratio in Table (2.4 instead of 4.4). The selectivity for isomerization (S(I) in Table 2) increases from 0.040 to 0.090 indicating that this reaction is less affected by the SMSI than hydrogenolysis. The selectivity for dehydrogenation is 26% after HTR.

Activation energies and turnover frequencies for sulfided and non-sulfided Pt/Al_2O_3 catalysts are also reported in Tables 1 and 2. In the MTR condition (sample 4), the Pt/Al_2O_3 catalyst exhibits higher values of the activation energy than the Pt/TiO_2 catalyst for the C–C terminal bond rupture (~185, i.e., + 20 kJ mol^{-1}) and for isomerization (271, i.e., + 75 kJ mol^{-1}). These are actually apparent activation energies which can be affected by the temperature at which one runs the reaction (*25*). That is the case for hydrogenolysis where the high coverage of hydrogen inhibits the reaction leading to a negative order of hydrogen in the rate law. One expects a decrease of the activation energy at higher temperature and lower hydrogen coverage. This could partially ex-

plain the deviation of -20 kJ mol^{-1}, since the reaction is performed at 580 K for Pt/TiO_2 catalyst instead of 540 K for Pt/Al_2O_3 catalyst. It is unlikely that this would explain a large shift for isomerization and, at the same time, a negligible one for middle-chain C–C bond rupture. In any case, the partial order in hydrogen stays negative in the SMSI state. Therefore, it seems that the lowering of H_2 coverage expected at higher temperature does not entirely explain the decrease in E_a. For similar reaction temperatures, platinum on alumina reduced at MTR or HTR conditions (samples 4 and 5), indeed exhibits very different E_a. The HTR-Pt/Al_2O_3 catalysts resemble more MTR-Pt/TiO_2 catalysts than MTR-Pt/Al_2O_3 although its hydrogenolysis activity is intermediate (1.7×10^{-2} molecule site^{-1} s^{-1}) between those of MTR-Pt on TiO_2 or Al_2O_3 (0.5×10^{-2} and 6.7×10^{-2} molecule site^{-1} s^{-1}, respectively).

Sulfidation of the catalyst before the reduction at 573 K (sample 6) also leads to a decrease of the activation energies compared to the unsulfided catalyst (sample 4). Activation energies lie in the range of the activation energies of HTR-Pt/Al_2O_3 catalyst and Pt/TiO_2 catalysts. The main effect resides in a strong depression, by three orders of magnitude, of the reaction rate which allows the observation of dehydrogenation with 19% selectivity (Table 2). The rates are comparable to the 0.44 wt% Pt/TiO_2 catalyst in the SMSI state: the turnover frequency for hydrogenolysis at 600 K is 3.6×10^{-5} and 8.5×10^{-5} molecule site^{-1} s^{-1} for MTR-I-S-Pt/Al_2O_3 and HTR-Pt/TiO_2 catalysts, respectively. The selectivity of the C–C terminal bond rupture is favored by the presence of sulfur (C_3/C_2 ~2) after MTR-I or HTR-I. A higher reduction temperature does not bring new properties as in the case of the unsulfided catalysts. Instead, one observes a decrease of the effect of sulfur, which can be removed from the catalysts as H_2S. In fact, strongly held sulfur is known to be removed only above 773 K in reducing condition, the sulfur level usually drops to a S/Pt molar ratio of 0.4–0.5 (*26, 27*), i.e., about half of the original amount (S/Pt = 0.8) introduced in our catalysts. An oxidation treatment at 623 K almost completely regenerates the original hydrogenolysis activity of the sulfur-free catalysts in the MTR-II condition. Nevertheless, the C_2 selectivity is not recovered (Table 2, $C_3/C_2 = 3.2$ instead of 0.75 for sample 4) and stays quite low. After a regeneration, a subsequent HTR treatment leads to the recovery of the dehydrogenation properties and to a drop by two orders of magnitude of hydrogenolysis. This is evidence that sulfur is not completely eliminated by the oxidative regeneration cycle and migrates from the support back onto the metal particle under strongly reducing condition (HTR). This is consistent with a recent study on strongly held sulfur (*28*).

The addition of sulfur and the effect of SMSI by migration of TiO_x moieties on the particles exhibit strong similarities; the extent of the depression of reaction rates, the increase of selectivity in isomerization and in middle-chain C–C bond rupture, the appearance of dehydrogenation activity, and the reversibility by oxidation treatment. The C_1/C_3 ratio stays close to one in all the experiments indicating that there is no significant shift of selectivity toward multiple or successive hydrogenolysis of *n*-butane.

DISCUSSION

Chemisorption Properties

After high temperature reduction, the ion-exchanged Pt/TiO_2 catalysts exhibit a strong inhibition of hydrogen chemisorption due to the SMSI state (*1*). One may be surprised that this is not the case for CO chemisorption. In fact, there is no CO chemisorption suppression because the reversible part of the CO chemisorption increases with reduction temperature (Fig. 1a). Hydrogen behaves differently, because the reversible contribution always remains low in the adsorption process. Therefore, the complete suppression of the irreversibly adsorbed hydrogen dominates the total hydrogen uptake in the SMSI state.

The main difference between H_2 and CO is due to the important contribution of the support to the reversible part of CO chemisorption. In fact, for pure TiO_2 heated under vacuum or under hydrogen pressure, a 37 kJ mol^{-1} differential heat of CO adsorption has been experimentally determined by Primet *et al.* (*29*). This adsorption, which does not occur on OH groups (*30*), can be attributed to anion vacancies created thermally. These defects are easier to create on TiO_2 where reduction of Ti^{4+} ions favors their formation by the removal of oxygen following the equation

$$Ti^{4+}\text{–}O\text{–}Ti^{4+} + H_2 \leftrightarrow Ti^{3+}\text{–}\square\text{–}Ti^{3+} + H_2O.$$

In polycrystalline TiO_2, rutile, or anatase, Ti^{3+} ions, generated under vacuum or under hydrogen pressure, have been characterized by EPR (*31*). On Rh/TiO_2 (*32*) and Pt/TiO_2 (*22, 33*) systems, the reduction of the support is catalytically activated by the metal in the vicinity of the metal, where Ti^{3+} ions are also characterized by EPR. In the case of Pt, a Ti_4O_7 phase has been characterized by transmission electron microscopy at the periphery of the metal particle (*34*). One of the Ti^{3+} ions, characterized by EPR and attributed to TiO_x moieties, is found to be involved in CO adsorption since its EPR signal disappears in the presence of CO (*22*). The adsorption of CO on the oxygen-deficient TiO_x moieties could account for the increase of the reversibly adsorbed CO. Such interaction of CO with the suboxide layer covering the metal in the SMSI state has been proposed by Vannice and Sudhakar to explain the promoting effect of TiO_2 on CO hydrogenation reactions (*35*).

Raupp and Dumesic (*36–38*) have studied the effect of the TiO_x coverage on polycrystalline Ni. They showed that the TiO_x species blocks CO adsorption sites and weakens CO adsorption strength. In contrast, the strength of hydrogen adsorption and the hydrogen coverage, based on available sites, increases. This effect, which increases the amount of H adatoms during CO hydrogenation, is sufficient to explain one or two orders of magnitude in the catalytic activity due to the support (*38*). On platinum, this seems not to be the case since our results show that the adsorption becomes reversible for both CO and H_2 in the SMSI state. A microcalorimetric study of H_2 adsorption is consistent with these results (*39*). On group VIII metals supported on TiO_2, other than nickel, calorimetry demonstrates that the initial as well as the average heat of adsorption of H_2 decreases by about 29 kJ mol^{-1} while for CO only the average heat of adsorption decreases by 20 kJ mol^{-1}. Therefore, unlike Ni, other group VIII metals will not exhibit a higher relative coverage of hydrogen when TiO_x species are present on their surfaces. An alternative explanation for the promotion effect of CO hydrogenation is given by Vannice and Sudhaker (*35*) for platinum. They propose that the adsorbed CO molecule interacts via its oxygen atom with the oxygen-deficient TiO_x moieties residing at the Pt surface. The CO dissociation may be assisted by the reoxidation of the TiO_x moieties. This is consistent with our EPR study of the Pt/TiO_2 system reduced in a medium range of reduction temperature where one of the Ti^{3+} ions in the close vicinity of the metal is irreversibly titrated by CO (*22*).

However, one must question the extent to which Ti^{3+} ions can exist under reaction conditions. Our own investigation of consumption of oxygen to reverse SMSI, induced by high temperature reduction, indicates that the oxygen released by CO hydrogenation on Rh/TiO_2 is quantitatively titrated by the Rh/TiO_x complex until SMSI is reversed (*11, 40*). Of course, it may still be possible to sustain the steady-state reaction with a very small quantity of Ti^{3+} at the steady state.

Effect of Impurities in the Support and Morphology of the Particles

Alumina is not a reducible oxide and aluminum has no stable suboxides. Nevertheless, an SMSI-like behavior has been ob-

served by some authors (*41*). This can be attributed to the presence of impurities like sulfate as shown in Pt/Al_2O_3 (*42*) or Rh/MgO catalysts (*43*). Upon high temperature reduction, sulfates are reduced to sulfur and migrate onto the particles. The reversibility of the effect of sulfur has been observed on H_2 chemisorption properties of sulfided Pt/Al_2O_3 catalysts where sulfur was deliberately introduced (*28*). The results on the *n*-butane reaction are consistent with this reversibility (compare, in Table 2, samples 6 and 8).

In the case of MTR-I-Pt/Al_2O_3, one may also expect chloride as an impurity and it could affect both H_2 and CO chemisorption and reaction of *n*-butane, particularly isomerization to isobutane which is known to be bifunctionally catalyzed by the Pt and the acidity imparted to the support by the chloride. Because it is expected that the chloride will be, in part, removed by the 773 K reduction (*26, 27*), the fact that reversible adsorption is about the same after HTR and MTR-II does not indicate any chloride effect. The total chemisorption of H_2 is somewhat lower on MTR-II than MTR, but not more than might be expected by some sintering after HTR. However, CO chemisorption is the same on MTR-II and MTR. When this isomerization of *n*-butane to isobutane is considered (compare sample 4 with 5 in Table 2) there is about an order of magnitude decrease in the rate of this reaction. Clearly this must be mostly due to changing the morphology of the Pt particles (evidenced by the decrease in chemisorption), but we cannot rule out the role of chloride impurity because, if there were a bifunctional component of the butane isomerization, removal of chloride by HTR would be expected to have a similar effect.

Though not as great as on TiO_2, a depression of H_2 chemisorption occurs (H/Pt decreases from 0.80 to 0.50) for the unsulfided Pt/Al_2O_3 catalyst at HTR conditions leading to an increase of the reversibly chemisorbed fraction. In the latter case, the activity for hydrogenolysis is decreased fourfold from its original value (Table 2). The characteristics of H_2 and CO chemisorption on HTR-Pt/Al_2O_3 catalysts are indeed comparable to those of the MTR-Pt/TiO_2 catalysts. For the latter, the loss of activity in hydrogenolysis is tenfold that of the unsulfided Pt/Al_2O_3 (compare, in Table 2, samples 1 or 3 with 4) and the activation energies comparable with those of the former. One may conclude that, on the high purity η-alumina used here, Pt particles after a HTR are in a similar state to that already experienced after MTR on TiO_2. The nature of this state is discussed below.

Recently, Vanslow and Mundshaum (*44*) have shown, by field emission microscopy, that the high-index planes are the first to be covered by TiO_x fragments, leaving the low-index plane available for catalysis. On a support one expects the same preference for the high-index planes to be covered. The fact that the activation energies do not change on Pt/TiO_2 after MTR or HTR conditions (Table 1, sample 1–3) indicates that the exposed surface is not changed. The particles have already experienced, at MTR conditions, a flattening previously observed by electron microscopy in HTR conditions (*34*), therefore leaving in both cases only low-index planes exposed. The increase of the heat of adsorption of benzene and the shift of the maximum rate of the hydrogenation of benzene toward high temperature on Pt/TiO_2 after HTR conditions has been attributed to this morphology change by Resasco *et al.* (*45*). These authors show that a similar morphology change does not occur for rhodium on TiO_2 at HTR conditions as well as for Pt/TiO_2 at LTR conditions. They claim that rhodium experiences a different SMSI effect as a result of the particle flattening occurring for platinum but not for rhodium. The self-diffusion rate of platinum atoms being larger than that of rhodium atoms can explain the different behavior.

Our results are consistent with the fact that platinum particles undergo a morphology change but, in addition, show that it does not occur only at high temperature but

already at MTR (573 K) on TiO_2. As a consequence, since the reference in the study of SMSI is always after LTR conditions, which in the case of platinum cannot be explored because of its low activity in hydrogenolysis, the SMSI effect could not be calibrated by MTR-Pt/TiO_2 catalysts. One should, instead, consider the MTR-Pt/Al_2O_3 catalysts as a better reference although it would be further improved by a chloride-free preparation. Therefore SMSI can be said to lead to a depression of three orders of magnitude for hydrogenolysis in the steady-state condition using MTR-Pt/Al_2O_3 as the reference, instead of 50 times as presented in the results section. Finally, the change of morphology described for MTR-Pt/TiO_2 catalysts occurs on a sulfur-free alumina after HTR.

Geometric and Electronic Effect

The effect of morphology, which is a geometric effect by nature, has been discussed previously on "normal" platinum. We describe here an approach to separate the effect of morphology, site blocking, and electronic effects on the kinetic parameters using compensation plots. These consist of a plot of the preexponential terms versus the activation energies, and the compensation is usually shown by a straight line on which lie all the points. Bond *et al.* have suggested that "*any family of catalysts exhibiting a simple compensation effect must possess active centers which are similar in their geometric and electronic architecture*" (*46*). Such compensations have been observed for hydrogenolysis reactions on different hydrocarbons over Ru (*47, 48*) and Rh (*49*) catalysts treated under different conditions. The curves must be plotted for each type of *n*-butane reaction taking place via a given active site.

The sites for hydrogenolysis and isomerization are composed of a critical reactant site (CRS) and a secondary site. The CRS concerns the hydrocarbon chemisorption mode (*50–53*) while the secondary site concerns the hydrogen chemisorption requirement to dehydrogenate the hydrocarbon (*51, 52*). On iridium, one distinguishes two pathways called an iso-unit mode and a C_2-unit mode, using a different number of surface atoms in the CRS (*50*). This has been demonstrated either by changing the size of the particles or by alloying iridium with gold (*51, 54*). The C_2-mode requires at least two surface metal atoms with a 170 kJ mol^{-1} activation energy and leads to middle-chain C–C bond rupture leading to the formation of ethane from *n*-butane. The iso-unit mode requires fewer (perhaps one) surface metal atoms with 250 kJ mol^{-1} activation energy and leads to formation of methane and propane from *n*-butane. Hydrogenolysis seems to occur via the same modes and on the same sites on both platinum and iridium. Nevertheless, some differences must be noted from the observations of our results. Contrary to what is observed on iridium, on platinum the iso-unit mode exhibits a lower

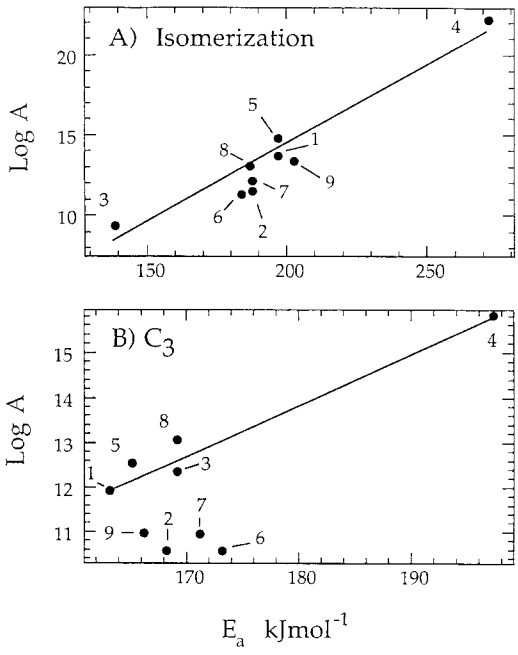

FIG. 4. Compensation curves for the formation of (A) isobutane and (B) propane from *n*-butane reactions on platinum supported on TiO_2 or Al_2O_3 after various pretreatment (see text)

TABLE 3

Characteristics of the Compensation Curves

Reactions	Slope of the compensation line[a]	Site blockage in Δ Log A[b]			
		SMSI[c]	MTR-I-S[c]	HTR-I-S[c]	HTR-II-S[c]
Isomerization	0.0976	−2.06	−1.8	−1.4	−1.6
C_1[d]	0.112	−1.92	−2.64	−2.12	−0.84
C_3[d]	0.113	−1.98	−2.55	−1.96	−1.36
C_2[d]	0.121	−2.06	−2.21	−2.06	−0.70

[a] Δ Log $A/\Delta E_a$ in the units of Tables 1 and 2, the preexponential factor in the units of TOF.
[b] Distance between the experimental point and the compensation line along the y axis in Fig. 4.
[c] SMSI concerns the HTR–Pt/TiO_2 sample and S concerns the sulfided Pt/Al_2O_3 samples.
[d] C_1, C_2, and C_3 refer to the reactions whose products are CH_4, C_2H_6, and C_3H_8, respectively.

activation energy (~160 kJ mol^{-1}) than the C_2-mode (~195 kJ mol^{-1}) and based on the activation energies, isomerization seems to occur mainly via the C_2-mode. In some cases, the isomerization seems to occur via a third mode with a higher E_a where the intermediate implies the formation of a π-complex as suggested previously (*55*).

In this study, the compensation behavior is, indeed, observed for each of the *n*-butane reactions on almost all the catalysts, as shown in Fig. 4. The compensation line has been calculated from a least-squares fit calculation based on the points corresponding to the catalysts reduced at MTR conditions (points 1, 3, 4, and 8), i.e., in the "normal state." Point 5, the HTR-Pt/Al_2O_3 catalyst, lies on the compensation line while some points (2, 6, 7, and 9) are below the line. These "odd points" correspond to platinum in the SMSI state or deeply poisoned by sulfur and correspond to the case of platinum suffering a strong site blockage, i.e., a decrease in the preexponential factor which correlates with site density. Table 3 reports some of the characteristics of the compensation behavior. The slope of the line in Δ Log $A/\Delta E_a$ is smaller for isomerization than for the terminal and middle C–C bond rupture. Since the most active catalysts have the highest activation energies for almost all of the hydrogenolysis reactions, the better the compensation the higher the preexponential factor, i.e., the smaller the slope of the compensation line. Following these considerations, the compensation efficiency is found to be higher for isomerization than for terminal C–C bond rupture and, finally, middle-chain C–C bond rupture. It appears that a smaller site requirement results in a better compensation efficiency.

For drastic changes due to surface poisoning or decoration, the extent of inhibition can be measured by the distance of the point off the compensation line. This inhibition is very similar for TiO_x decoration and sulfur poisoning. The main effect in both cases is therefore a mere site blocking. The slight preference of sulfur to poison the iso-unit mode (Table 3, Δ Log A ~ −2.6 instead of ~ −2) at high surface coverage (MTR-I-S) could be due to an electronic effect, but one could also argue that sulfur can preferentially block the site required for the iso-unit mode, i.e., edges and corners where this mode preferentially operates.

Site Blockage and Reaction Self-Poisoning

Finally, this comparison between sulfur poisoning and the effect of SMSI brings us to other similarities which were evidenced by other authors: decoration of the surface of a particle by fragments of the support and

formation of alloys leading to the dilution of the active atoms (Pt, Rh, Ir, Ni, etc.) with an inactive metal (Cu, Ag, Au, etc.) (*4*) or the alloying effect just described and reaction self-poisoning by carbonaceous depositions (*56–58*). The carbonaceous deposition effectively occurs on our samples and has been characterized on the Arrhenius plot for each reaction by two straight lines on which lie two sets of points collected at different data acquisition conditions. The first set of data was taken by increasing the temperature between each couple of measurements performed at the steady state and the second, following the first set, by decreasing the temperature. The deactivation is evidenced by a smaller rate in the second set of data leading to a higher apparent activation energy. This activation energy difference is a qualitative measure of the importance of the self-poisoning.

The difference in activation energy between the two sets of results is always small ($< +20$ kJ mol^{-1}) for all the catalysts of Tables 1 and 2, the worst catalyst being MTR-II-Pt/TiO_2 which exhibits a high C_1/C_3 ratio (Table 2, sample 3). This deactivation is found to be very important for the 1 wt% Pt/TiO_2 catalysts ($\Delta E_a \sim 90$ kJ mol^{-1}) whose results, for this reason, have not been reported here. This is consistent with the fact that larger particles are more easily self-poisoned (*56–58*). The latter catalyst has, indeed, a smaller TOF than the 0.44 wt% Pt/TiO_2 at the same conditions. The drop in activity due to reaction self-poisoning is not as drastic as for the other inhibitor effects cited previously. At the temperature of reaction, which is high for platinum, the carbon may rearrange on the surface and leave large patches of non-affected surface as proposed by Ponec and co-workers (*56–58*).

This qualitative analysis reinforces the view that hydrocarbon skeleton rearrangements, which occur on ensembles of surface atoms, are mainly inhibited via geometric effects such as morphology modification or, to a larger extent, by site blockage. This mechanism seems to operate roughly in a similar manner whatever the nature of the adatom or species introduced on or in the surface (sulfur, carbonaceous residues, group IB metal atom, TiO_x fragments, etc.). These inhibition effects would appear to be, to a first order, independent and additive.

CONCLUSION

Surface inhibition effects by sulfur poisoning or strong metal-support interaction, are compared on small particles supported on alumina or titania. The change in properties is monitored by either hydrogen or carbon monoxide chemisorption at room temperature or by *n*-butane hydrogenolysis and isomerization. Both effects appear at high temperature in a hydrogen atmosphere (HTR conditions). They are attributed to the migration of sulfur and TiO_x suboxide fragments of the support onto the particle surface. These species are formed by reduction of either the sulfate located on the support or the support itself, respectively. As a consequence, the irreversible part of the chemisorbed hydrogen and carbon monoxide, which titrates the metal surface, is completely suppressed.

The reversible part of chemisorption is maintained only for CO and increases for the low metal loaded sample (0.44 wt%). This is attributed to the adsorption of this molecule on Ti^{3+} ions and oxygen vacancies created in the proximity of the Pt particles at HTR. After a medium temperature of reduction (573 K) of Pt/TiO_2, the platinum experiences a slight decrease of chemisorption capacity. This intermediate state, which can be generated on pure alumina only at high temperature, is evidenced by (i) decrease by a factor of 10 and four times on TiO_2 and Al_2O_3 supports, respectively, from the original activity of the Pt/Al_2O_3 catalyst after a 513 K reduction, the latter being taken as the reference. For both supports, a decrease of activation energies, in particular for isomerization and, to a lesser extent, for C–C terminal bond rupture is observed. This is attributed to a change

of particle morphology which consists of a flattening caused by wetting the support and exposing to the gas phase less active low-index Pt planes. One notes that in the presence of sulfur, this intermediate state is achieved only at MTR, as on TiO_2.

Hydrogen chemisorption on sulfided Pt/Al_2O_3 catalyst, as shown in the literature (*28*), is quite similar to that on Pt/TiO_2 catalysts. For the strongest sulfur inhibition and for SMSI after high temperature reduction inhibition of activity (drop of three orders of magnitude in hydrogenolysis activity) can be explained by a simple site blocking. The differences between rhodium, iridium, and platinum may partially reside in the change of morphology which primarily occurs for platinum particles. Inhibition of surface properties seems, therefore, to be quite similar and independent of its origin, i.e., whether it results from the SMSI state, sulfur poisoned surfaces, alloying with an inactive metal or carbonaceous deposition in self-poisoned reactions. In all cases, the geometric effect appears to dominate for these structure sensitive reactions.

ACKNOWLEDGMENTS

This work was supported by the US Department of Energy, Office of Basic Energy Science, under contract DE-AC02-81-ER10829. We also thank NSF/CNRS for support from the US–France Cooperative Science Program which made possible the cooperation between our two laboratories while one of us, L.B., was appointed by the CNRS at the Laboratorie de Réactivité de Surface et de Structure, Université P. et M. Curie, Paris, and the NSERC of Canada for the continuation of the support.

REFERENCES

1. Tauster, S. J., Fung, S. C., and Garten, R. L., *J. Am. Chem. Soc.* **100,** 170 (1978).
2. Imelik, B., Naccache, C., Coudurier, G., Praliaud, H., Mériaudeau, P., Martin, G. A., and Védrine, J. C., Eds. "Metal Support and Metal Additive Effect of Catalysis," *Stud. Surf. Sci. Catal.*, Vol. 11. Elsevier, Amsterdam, 1982.
3. Santos, J., Phillips, J., and Dumesic, J. A., *J. Catal.* **81,** 147 (1983).
4. Resasco, D. E., and Haller, G. L., *J. Catal.* **82,** 279 (1983).
5. Levin, M., Salmeron, M., Bell, A. T., and Somorjai, G. A. , *Surf. Sci.* **160,** 123 (1986).
6. Sadeghi, H. R., and Henrich, V. E., *J. Catal.* **87,** 279 (1984); *Appl. Surf. Sci.* **19,** 330 (1984).
7. Dwyer, D. J., Robbins, J. L., Cameron, S. D., Dudash, N., and Hardenberg, J., *ACS Symp. Ser.* **298,** 21 (1986).
8. Dwyer, D. J., Cameron, S. D., and Gland, J., *Surf. Sci.* **159,** 430 (1985).
9. Vannice, M. A., and Garten, R. L., *J. Catal.* **56,** 236 (1979); *J. Catal.* **63,** 255 (1980).
10. Morris, S., R., Moyes, R. B., and Wells, P. B., *Stud. Surf. Sci. Catal.* **11,** 247 (1982).
11. Huang, H., Ph.D. thesis, Yale University, 1986.
12. Baker, R. T. K., Kim, K. S., Emerson, A. B., and Dumesic, J. A., *J. Phys. Chem.* **90,** 860 (1986).
13. Resasco, D.E., and Haller, G. L., *J. Phys. Chem.* **88,** 4552 (1984).
14. Sinfelt, *Catal. Rev.-Sci. Eng.* **3,** 175 (1969); *in* "Advances in Catalysis" (D. D. Eley, H. Pines, and P. B. Weisz, Eds.), Vol. 23, p. 91. Academic Press, New York, 1973.
15. Haensel, V., and Sterba, M., *J. Ind. Eng. Chem. Prod. Res. Dev.* **15,** 3 (1976); Menon, P. G., and Prasad, J., *in* "Proceedings, 6th International Congress on Catalysis, London, 1976" (G. C. Bond, P. B. Wells, and F. C. Tompkins, Eds.), Vol. 2, p. 1061. The Chemical Society, London, 1976.
16. Biloen, P., Helle, J. N., Verbeerk, H., Dautzenberg, F. M., and Sachtler, W. M., H., *J. Catal.* **63,** 112 (1980).
17. Oudar, J., *Catal. Rev.-Sci. Eng.* **22,** 171 (1980).
18. Sadeghi, H. H., and Henrich, V. E., *J. Catal.* **109,** 1 (1988).
19. Horsley, J. A., *J. Am. Chem. Soc.* **101,** 2877 (1979).
20. Haberlandt, H., and Ritschl, F., *J. Phys. Chem.* **90,** 4322 (1986).
21. Yang, L., Rong, C., Guoxing, X., and Hongli, W., *J. Mol. Catal.* **42,** 337 (1987).
22. Bonneviot, L., and Haller, G. L., *J. Catal.* **113,** 96 (1988).
23. Haller, G. L., Resasco, D. E., and Rouco, A. J., *Faraday Discuss., Chem. Soc.* **72,** 109 (1982).
24. Resasco, D., and Haller, G. L., *Stud. Surf. Sci. Catal.* **11,** 105 (1982).
25. Bond, G. C., "Heterogeneous Catalysis Principles and Applications," 2nd ed., p. 54. Clarendon Press, Oxford, 1987.
26. Apesteguia, C., Garetto, T., Brema, C., and Parera, J. M., *Appl. Catal.* **10,** 291 (1984).
27. Barbier, J., Marecot, P., Tifouti, L., Guenin, M., and Frety, R., *Appl. Catal.* **19,** 375 (1985).
28. Apesteguia, C. R., Garetto, T. F., and Borgna, A., *J. Catal.* **106,** 73 (1987).
29. Primet, M., Bandiera, J., Naccache, C., and Mathieu, M. V., *J. Chim. Phys.* **67,** 535 (1970).
30 Yates, D. J. C., *J. Phys. Chem.* **65,** 746 (1961).
31. Mériaudeau, P., Che, M., Gravelle, P. C., and Teichner, S. J., *Bull. Soc. France,* 13 (1971).
32. Conesa, J. C., Malet, P., Munuera, G., Sanz, J., and Soria, J., *J. Phys. Chem.* **88,** 2986 (1984).

33. Huizinga, T., and Prins. R., *J. Phys. Chem.* **85,** 2156 (1981).
34. Baker, R. T. K., Prestridge, E. B., and Garten, R. L., *J. Catal.* **59,** 293 (1979); **56,** 390 (1979).
35. Vannice, M. A., and Sudhakar, C., *J. Phys. Chem.* **88,** 2429 (1984).
36. Raupp, G. B., and Dumesic, J. A., *J. Phys. Chem.* **88,** 660 (1984).
37. Raupp, G. B., and Dumesic, J. A., *J. Catal.* **95,** 587 (1985).
38. Raupp, G. B., and Dumesic, J. A., *J. Catal.* **96,** 597 (1985).
39. Hermann, J. M., Gravelle-Rumeau-Maillot, M., and Gravelle, P. C., *J. Catal.* **104,** 136 (1987).
40. Haller, G. L., and Resasco, D. E., *in* "Advances in Catalysis" (D. D. Eley, H. Pines, and P. B. Weisz, Eds.), Vol. 36, p. 173. Academic Press, San Diego, 1989.
41. Dautzenberg, F., M., and Wolters, *J. Catal.* **51,** 26 (1979).
42. Kunimori, K., Ikeda, Y., Coma, M., and Uchijima, T., *J. Catal.* **79,** 185 (1983).
43. Wang, J., Lercher, J. A., and Haller, G. L., *J. Catal.* **88,** 18 (1984).
44. Vanslow, R., and Mundschaum, M., *J. Catal.* **103,** 426 (1987).
45. Resasco, D. E., Fenoglio, R. J., Suarez, M. P., and Cechini, J. O., *J. Phys. Chem.* **90,** 4330 (1986).
46. Bond, G. C., Rajaram, R. R., and Burch, R., *J. Phys. Chem.* **90,** 4877 (1986).
47. Burch, R., Bond, G. C., and Rajaram, R. R., *J. Chem. Soc., Faraday Trans. 1* **82,** 1985 (1986).
48. Anderson, J. B. F., Burch, R., and Cairns, J. A., *J. Chem. Soc., Faraday Trans. 1* **83,** 913 (1987).
49. Anderson, J. R., *in* "Advances in Catalysis" (D. D. Eley, H. Pines, and P. B. Weisz, Eds.), Vol. 23, p. 1. Academic Press, New York, 1973.
50. Anderson, J. R., *Prep. Am. Chem. Soc. Petr. Div.* **26,** 361 (1981).
51. Frennet, A., Lienard, G., Crucq, F., and Degols, F., *J. Catal.* **53,** 150 (1978).
52. Martin, G. A., *J. Catal.* **60,** 345 (1979).
53. Foger, K., and Anderson, J. R., *J. Catal.* **59,** 325 (1979); **64,** 448 (1980).
54. Boudart, M., Aldag, A. W., and Ptak, L. D., *J. Catal.* **11,** 35 (1968).
55. Karpinski, Z., and Clarke, J. T. A., *J. Chem. Soc. Faraday Trans.* **71,** 2310 (1975); Weisang, F., Gault, F, *J. Chem. Soc. Chem. Commun.*, 519 (1979); de Jongste, H. C., and Ponec, V., *J. Catal.* **64,** 228 (1980).
56. Vogelzang, M. W., and Ponec, V., *J. Catal.* **111,** 77 (1988).
57. Vogelzang, M. W., Boltman, M. J. P. and Ponec, V., *Faraday Discuss., Chem. Soc.*, **72,** 33 (1981).
58. Lankhorst, P., P., de Jongste, H., C. and Ponec, V. *in* "Catalysts Deactivation," B. Delmon and F. Froment Eds., p. 43, Elsevier, Amsterdam, 1980.